Electrochemistry

DOI: 10.1002/anie.201301084

In situ Seamless Magnetic Measurements for Solid-State Electrochemical Processes in Prussian Blue Analogues**

Tetsuya Yamada, Kantaro Morita, Heng Wang, Keita Kume, Hirofumi Yoshikawa, and Kunio Awaga**

Solid-state electrochemistry is a wide research area covering various topics from fundamental sciences to applications.[1] At present, one of the most important goals is to develop high-performance rechargeable batteries.[2,3] We recently developed a new type of rechargeable battery, the molecular cluster battery (MCB), which consists of molecular clusters such as Mn12 clusters ($[Mn_{12}O_{12}(RCOO)_{16}(H_2O)_4]$, $R = CH_3$, C_6H_5, etc.)[4–6] and polyoxometalates (POMs, $[PMo_{12}O_{40}]^{3-}$),[7–9] as cathode active materials and a lithium metal as an anode. It was found that MCBs can exhibit higher battery capacities than conventional lithium ion batteries.[2] In operando XAFS studies on MCBs of Mn12 and POMs revealed that they exhibit 8-[5,6] and 24-electron reductions[7] during discharge, respectively. It is notable that such super-reduced species ($[Mn12]^{8-}$ and $[POM]^{27-}$) are new materials that can be obtained only by solid-state electrochemistry.[5,7,10] In other words, conventional solution electrochemistry cannot produce these species in the electrochemical windows of solvents, because redox species in solutions are well-stabilized by solvation. It is expected that such electrochemically super-reduced compounds would exhibit novel physicochemical properties.

Various magnetic properties of Prussian blue analogues (PBAs), such as photomagnetism,[11] room-temperature ferrimagnetism,[12] spin crossover[13] and so on,[14] have been reported in the last two decades. Solid-state electrochemical techniques are useful for modulating their magnetic properties. Sato et al. prepared thin films of $[Cr^{II}_{1.29}Cr^{III}_{1.14}(CN)_6]^0$ by electrochemical deposition, which exhibits a ferrimagnetic ordering at $T_C = 240$ K. They found a significant (100 K) decrease in T_C, after a potentiostatic reduction of this compound to $[Cr^{II}_{1.29+x}Cr^{III}_{1.14-x}(CN)_6]^{x-}$.[15] Recently, Okubo et al. fabricated a lithium battery, whose cathode active material was $K_{0.14}Cu^{II}_{1.43}[Fe^{III}(CN)_6]$. Although this compound exhibits a ferromagnetic ordering at 20 K, this transition disappeared when the battery was discharged galvanostatically.[16] As these measurements were performed by ex situ methods, the samples were exposed to air and little information was obtained about the intermediate states during reductions (discharges). Therefore, in situ magnetic analyses are necessary to seamlessly reveal the electrochemically controlled magnetic properties of the PBAs.

Herein, we developed an in situ magnetic measurement system under solid-state electrochemical reactions, and applied it to a mixed-valent chromium PBA ferrimagnet with a high T_C of 215 K. We describe a seamless change in magnetism during an electrochemical reduction of this compound, and discuss the correlation between the spin states of the Cr ions and the bulk magnetism.

Figure 1 shows the battery cell for in situ magnetic measurements. Its size is $15 \times 7 \times 5$ mm^3, so that it can fit inside a commercial SQUID susceptometer (Quantum Design MPMS). The outside jacket is made of quartz. This small battery cell consists of an anode (Li metal), a separator (Whatman no. 1820-125), and a cathode including the PBA. The Pt foils on both sides of the cell are current collectors. The cathode was prepared as follows: the PBA (10 wt%) and conductive carbon black (70 wt%) were mixed with polyvinylidene difluoride (PVDF, 20 wt%) as a binder, and then the mixture was spread onto an aluminum plate and dried.

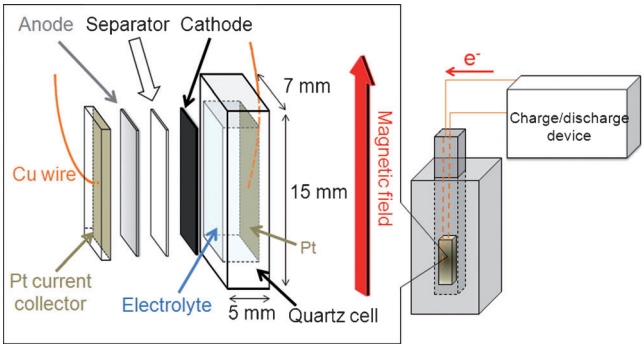

Figure 1. View of a lithium battery cell for in situ magnetic measurements. The anode is made of lithium metal. The cathode is a mixture of the Prussian blue analogue, conductive carbon black, and PVDF. The separator is a glass microfiber filter. This cell can be inserted into a SQUID device for magnetic measurements.

[*] Dr. T. Yamada, K. Morita, Dr. H. Wang, K. Kume, Dr. H. Yoshikawa, Prof. K. Awaga
Department of Chemistry and Research Centre for Materials Science, Nagoya University
Furo-cho, Chikusa, 464-8602 Nagoya (Japan)
E-mail: yoshikawah@mbox.chem.nagoya-u.ac.jp
awaga@mbox.chem.nagoya-u.ac.jp
Dr. T. Yamada, Prof. K. Awaga
CREST, JST
Furo-cho, Chikusa, 464-8602 Nagoya (Japan)

[**] This work was performed with the approval of PF PAC (Proposal Nos. 2008G586, 2009G528, 2010G557, and 2012G027). We are grateful to the Ministry of Education, Culture, Sports, Science, and Technology (MEXT) of Japan for a Grant-in-Aid for Scientific Research. We would like to thank Prof. Michel Verdaguer, from Université Pierre-et-Marie-Curie, for his helpful discussions.

Supporting information for this article is available on the WWW under http://dx.doi.org/10.1002/anie.201301084.

The battery cell was fabricated with an electrolyte of $LiPF_6$ and a mixed solution of diethyl carbonate (DEC) and ethylene carbonate (EC) (DEC/EC = 1:1) in an Ar atmosphere. The cell was connected to a charge–discharge device (Hokuto HJ1001-SM8A), and then inserted into the SQUID. In situ magnetic measurements were performed as follows: the battery of the PBA was charged or discharged by leading or taking out, respectively, a constant current density of 0.1 mA cm^{-2} in the SQUID at room temperature. At specific voltages versus lithium, we opened the circuit to keep the voltage constant and carried out variable-temperature magnetic measurements under a field of 10 kOe. The field dependence of the magnetization was also examined at constant voltages.

The mixed-valent Cr PBA used as a cathode active material was prepared by mixing aqueous solutions of $Cr^{II}Cl_2{\cdot}6H_2O$ and $K_3[Cr^{III}(CN)_6]$ according to the literature.[17] The obtained PBA was characterized by elemental analysis, ICP, IR, TGA, powder X-ray diffraction (PXRD), and magnetic data (see the Supporting Information). The results indicate a chemical formula of $Cr^{II}_{1.91}Cr^{III}_{0.33}[Cr^{III}(CN)_6]{\cdot}\chi_{1.24}Cl_{0.13}(OH)_{1.68}{\cdot}5.25\,H_2O$, in which the A site with strong ligand field is occupied by Cr^{II} ($S = 2$) and Cr^{III} ($S = 3/2$), and the B site with weak ligand field site by Cr^{III} ($S = 3/2$) (Figure 4, inset). Using this sample, the battery cells were prepared by the method described above. Before the magnetic measurements, the electrochemical processes were examined by battery-performance tests and in operando Cr K-edge XANES measurements. Figure 2a shows the first discharge, in which the battery voltage is plotted as a function of time (see also the Supporting Information, Figure S5). The voltage shows a gradual decrease from 4.2 to 1.5 V. The battery capacity at 1.5 V corresponds to 150 Ah/kg. The results of the in operando Cr K-edge XANES studies are shown in the Supporting Information, Figure S6. It is found that the edge energy, which is correlated to the valence of the Cr ions, depends little on the battery voltage above 2.5 V and shows a decrease below it. This means that there is no electrochemical reaction in the voltage range above 2.5 V; the gradual voltage decrease above 2.5 V in the discharge curve is probably caused by a capacitance effect, which is characteristic of MCBs, as discussed before.[5,6] The number of electron implied during discharge from 2.5 to 1.7 V is estimated to be 1.33 (see Eq. (S1) in the Supporting Information).

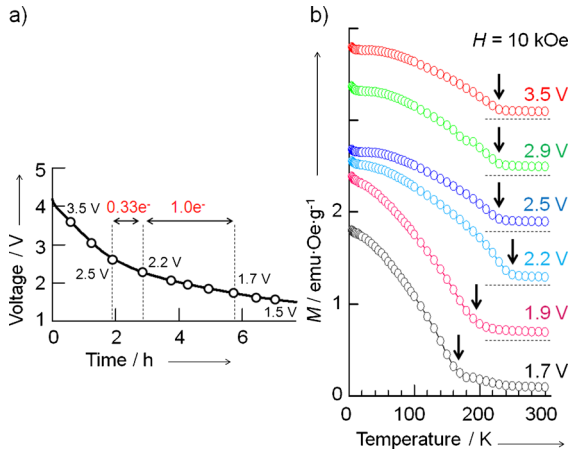

Figure 2. a) The first discharge curve of the mixed-valent chromium PBA battery. The open circles indicate the voltages at which magnetism was measured. b) Temperature dependence of the magnetization for the Cr PBA in the Li batteries at various voltages during discharge. The arrows, indicating quick rises in magnetization, are only guides for the eyes.

Figure 2b shows the evolution of the temperature dependences of the magnetization for the PBA at various voltages during discharge. These magnetization values were obtained by subtracting the background contributions from the quartz cell, Pt current collectors, and lithium metal. The temperature dependence of the magnetization in the voltage range of 3.5–2.5 V exhibits a quick rise below 215 K. This behavior is the same as that of the initial sample (Supporting Information, Figure S7), and the change at 215 K is assigned to a ferrimagnetic transition. This behavior is also similar to that reported for a mixed-valent Cr PBA.[15,17] In this voltage range, there is no change in temperature dependence of the magnetization. This is consistent with the results of XANES, namely no electrochemical reaction above 2.5 V. As the voltage decreases from 2.5 V, the transition temperature appears to increase up to 2.2 V and to decrease significantly below that. To evaluate the transition temperature T_C more precisely, we carried out Arrott plot analysis (Supporting Information, Figure S9). Figure 3a,b shows the voltage dependence of T_C and the magnetization M at 2 K. While the values of T_C and M(2 K) depend little on the battery voltage above 2.5 V, T_C is shifted by 15 K toward the high-temperature side at 2.2 V. Then, the voltage decrease from 2.2 to 1.7 V causes a T_C drop to 150 K with a significant increase of M(2 K) (Supporting Information, Figure S8).

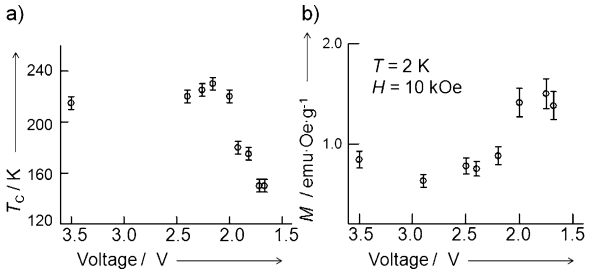

Figure 3. Voltage dependence of a) T_C and b) magnetization at 2 K.

The magnetization curves at 2 K at the representative voltages of 3.5, 2.2, and 1.7 V are shown in the Supporting Information, Figure S10 (see also Figure S11). At these voltages, the magnetization curves exhibit coercive fields, which are consistent with a behavior of ferrimagnet. The voltage dependence of the coercive field H_c is shown in the Supporting Information, Figure S10. The value of H_c gradually increases below 2.5 V, peaking at 1.7 V, which is probably due to a larger magnetic anisotropy of Cr^{II} ions. These magnetic properties are reproducible and reversible in the charge/discharge processes above 1.7 V (Supporting Informa-

tion, Figure S12), and they present no more long range order, which is probably due to their structural decomposition below this voltage. This is confirmed by the PXRD measurements (Supporting Information, Figures S8, S13).

The observed electrochemical magnetic processes can be explained in Figure 4. This shows the expected valences of the Cr ions and their spin at the A and B sites, in the battery voltage range from 3.5 to 1.7 V. Between 3.5 and 2.5 V, the A site is occupied by Cr^{II} ($S_A = 2$) and Cr^{III} ($S_A = 3/2$), while the B site is occupied by Cr^{III} ($S_B = 3/2$). This state is the same as that of the pristine sample, $Cr^{II}_{1.91}Cr^{III}_{0.33}[Cr^{III}(CN)_6]$, where the parts of vacancy χ, Cl^-, OH^-, and H_2O are omitted. During discharge from 2.5 to 2.2 V, the change in battery capacity indicates a 0.33-electron reduction (Figure 2a) to $Cr^{II}_{2.24}[Cr^{III}(CN)_6]$, as it is well-known that the redox potential of N,O-coordinated Cr^{III} is higher than that of C-coordinated Cr^{III} (see the Supporting Information). When the battery voltage changes from 2.2 to 1.7 V during discharge, the capacity change corresponds to a one-electron reduction. It is reasonable to assign this redox change to the reduction of the Cr^{III} ions at the B site, namely to $Cr^{II}_{2.24}[Cr^{II}(CN)_6]$.

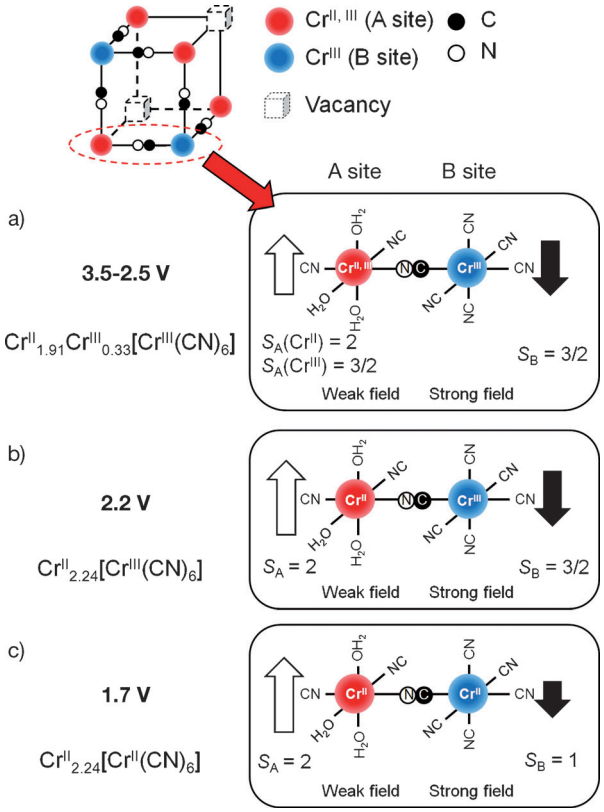

Figure 4. Structure of the mixed-valent chromium PBA and the expected valences and spin states of the Cr ions at a) 3.5–2.5 V, b) 2.2 V, and c) 1.7 V during discharge. The Cr ions at the A and B site are coordinated to the cyanide by N and C atoms, respectively.

Table 1 summarizes the chromium valences and the magnetic parameters at 2.5, 2.2, and 1.7 V. S_T is the total spin quantum number, which was calculated under the assumption of an antiferromagnetic interaction between the spins at the A and B sites, namely S_A and S_B, respectively. The values of S_T show a gradual increase during discharge and explain the monotonous increase of the magnetization (Figure 3b). The Curie temperatures of the PBAs can be calculated by S_A, S_B, and the magnetic coupling constant J between them, based on the mean-field theory.[18] As the change of J is negligible during the discharge in the present case (see the Supporting Information), the Curie temperatures T_C^{calc} at 2.2 and 1.7 V are calculated with the parameters S_A, S_B, and T_C at 2.5 V (see Eq. (S8) in the Supporting Information). As shown in Table 1, the voltage dependence of T_C can be reproduced by T_C^{calc}. These analyses indicate that the magnetic properties of the mixed-valent chromium PBA can be seamlessly explained by the valence and spin-state changes. In other words, solid-state electrochemistry is a useful method for controlling the valence states of the PBAs and can produce peculiar magnetic properties.

Table 1: The chromium valences and the magnetic parameters of the PBA at 2.5 V, 2.2 V, and 1.7 V during discharge.

	A site Valence	S_A	B site Valence	S_B	S_T	T_C [K]	T_C^{calc} [K]
2.5 V	1.91Cr^{II} 0.33Cr^{III}	2 3/2	1Cr^{III}	3/2	2.8	215	–
2.2 V	2.24Cr^{II}	2	1Cr^{III}	3/2	3.0	230	222
1.7 V	2.24Cr^{II}	2	1Cr^{II}	1	3.5	150	162

In summary, we have developed in situ magnetic measurements in an electrochemical environment and applied them to mixed-valent chromium PBA. A continuous redox change of the PBA was obtained by solid-state electrochemistry in the voltage range of 2.5 to 1.7 V, and seamless magnetic analysis was successful. It was revealed that the magnetic properties, such as M(2K) and T_C, can be well understood by the two-step redox and spin changes at the A and B sites. This kind of in situ magnetic measurement will open new avenues in the research fields of electrochemistry, coordination chemistry, and solid-state physics toward discovering novel magnets prepared by solid-state electrochemical reactions.

Received: February 6, 2013
Published online: April 25, 2013

Keywords: electrochemistry · lithium batteries · magnetic properties · Prussian blue analogues · redox chemistry

[1] a) B. O'Regan, M. Gratzel, *Nature* **1991**, *353*, 737; b) T. Fujimoto, M. M. Matsushita, K. Awaga, *J. Phys. Chem. C* **2012**, *116*, 5240; c) Y. Miyoshi, K. Takahashi, T. Fujimoto, H. Yoshikawa, M. M. Matsushita, Y. Ouchi, M. Kepenekian, V. Robert, M. P. Donzello, C. Ercolani, K. Awaga, *Inorg. Chem.* **2012**, *51*, 456; d) I. Valov, I. Sapezanskaia, A. Nayak, T. Tsuruoka, T. Bredow, T. Hasegawa, G. Staikov, M. Aono, R. Waser, *Nat. Mater.* **2012**, *11*, 530.
[2] S. Whittingham, *Chem. Rev.* **2004**, *104*, 4271.
[3] a) T. Sakai, I. Uehara, H. Ishikawa, *J. Alloys Compd.* **1999**, *293–295*, 762; b) H. Kitaura, Z. Zhou, *Energy Environ. Sci.* **2012**, *5*, 9077; c) I. Kowalczk, J. Read, M. Salomon, *Pure Appl. Chem.* **2007**, *79*, 851; d) Y. Morita, S. Nishida, T. Murata, M. Moriguchi,

A. Ueda, M. Satoh, K. Arifuku, K. Sato, T. Takui, *Nat. Mater.* **2011**, *10*, 947.
[4] H. Yoshikawa, C. Kazama, K. Awaga, M. Satoh, J. Wada, *Chem. Commun.* **2007**, 3169.
[5] H. Wang, S. Hamanaka, T. Yokoyama, H. Yoshikawa, K. Awaga, *Chem. Asian J.* **2011**, *6*, 1074.
[6] H. Yoshikawa, S. Hamanaka, Y. Miyoshi, Y. Kondo, S. Shigematsu, N. Akutagawa, M. Sato, T. Yokoyama, K. Awaga, *Inorg. Chem.* **2009**, *48*, 9057.
[7] H. Wang, S. Hamanaka, Y. Nishimoto, S. Irle, T. Yokoyama, H. Yoshikawa, K. Awaga, *J. Am. Chem. Soc.* **2012**, *134*, 4918.
[8] N. Kawasaki, H. Wang, R. Nakanishi, S. Hamanaka, R. Kitaura, H. Shinohara, T. Yokoyama, H. Yoshikawa, K. Awaga, *Angew. Chem.* **2011**, *123*, 3533; *Angew. Chem. Int. Ed.* **2011**, *50*, 3471.
[9] H. Wang, N. Kawasaki, T. Yokoyama, H. Yoshikawa, K. Awaga, *Dalton Trans.* **2012**, *41*, 9863.
[10] a) R. Bagai, G. Christou, *Inorg. Chem.* **2007**, *46*, 10810; b) K. Maeda, S. Himeno, T. Osakai, A. Saito, T. Hori, *J. Electroanal. Chem.* **1994**, *364*, 149.
[11] a) O. Sato, T. Iyoda, A. Fujishima, K. Hashimoto, *Science* **1996**, *272*, 704; b) N. Shimamoto, S. Ohkoshi, O. Sato, K. Hashimoto, *Chem. Lett.* **2002**, 486; c) S. Margadonna, K. Prassides, A. N. Fitch, *Angew. Chem.* **2004**, *116*, 6476; *Angew. Chem. Int. Ed.* **2004**, *43*, 6316; d) S. Ohkoshi, K. Hashimoto, *J. Am. Chem. Soc.* **1999**, *121*, 10591.
[12] a) S. Ferlay, T. Mallah, R. Ouahes, P. Veillet, M. Verdaguer, *Nature* **1995**, *378*, 701; b) O. Hatlevik, W. E. Buschmann, J. Zhang, J. L. Manson, J. S. Miller, *Adv. Mater.* **1999**, *11*, 914; c) S. M. Holmes, S. G. Girolami, *J. Am. Chem. Soc.* **1999**, *121*, 5593; d) E. Dujardin, S. Ferlay, X. Phan, C. Desplanches, C. C. Moulin, P. Saintavict, F. Baudelet, E. Dartyge, P. Veillet, M. Verdaguer, *J. Am. Chem. Soc.* **1998**, *120*, 11347.
[13] a) W. Kosaka, K. Nomura, K. Hashimoto, S. Ohkoshi, *J. Am. Chem. Soc.* **2005**, *127*, 8590; b) M. Nishino, K. Boukheddaden, S. Miyashita, F. Varret, *Phys. Rev. B* **2005**, *72*, 064452.
[14] a) S. Ohkoshi, K. Arai, Y. Sato, K. Hashimoto, *Nat. Mater.* **2004**, *3*, 857; b) V. Ksenofontov, G. Levchenko, S. Reiman, P. Gütlich, *Phys. Rev. B* **2003**, *68*, 024415; c) E. Coronado, M. C. Giménez-López, T. Korzeniak, G. Levchenko, F. M. Romero, A. Segura, V. García-Baonza, J. C. Cezar, F. M. F. de Groot, A. Milner, M. Paz-Pasternak, *J. Am. Chem. Soc.* **2008**, *130*, 15519.
[15] O. Sato, T. Iyoda, A. Fujishima, K. Hashimoto, *Science* **1996**, *271*, 49.
[16] M. Okubo, D. Asakura, Y. Mizuno, T. Kudo, H. Zhou, A. Okazawa, N. Kojima, K. Ikedo, T. Mizokawa, I. Honma, *Angew. Chem.* **2011**, *123*, 6393; *Angew. Chem. Int. Ed.* **2011**, *50*, 6269.
[17] a) T. Mallah, S. Thiébaut, M. Verdaguer, P. Veillet, *Science* **1993**, *262*, 1554; b) S. S. Kaye, H. J. Choi, J. R. Long, *J. Am. Chem. Soc.* **2008**, *130*, 16921.
[18] L. Néel, *Ann. Phys. (Paris)* **1948**, *3*, 137.

